

# Fatigue Strength of Crack-Healed Si<sub>3</sub>N<sub>4</sub> at Elevated Temperature

K. ANDO,<sup>1</sup> F. YAO,<sup>1</sup> M. C. CHU,<sup>1</sup> and S. SATO<sup>2</sup>

<sup>1</sup>Department of Energy & Safety Engineering, Yokohama National University, 79-5, Hodogaya, Yokohama, 240-8501 Japan.

<sup>2</sup>NHK Spring, 3-10 Fukuura, Kanazawaku, Yokohama, Japan

**ABSTRACT:** *Si<sub>3</sub>N<sub>4</sub>/SiC composite ceramics were sintered to investigate their fatigue strength behavior after crack healing. Y<sub>2</sub>O<sub>3</sub> and Al<sub>2</sub>O<sub>3</sub> powders were added as sintering additives to enhance the sintering properties. A three-point bending specimen (sized 3 × 4 × 40mm) was hewed out from a sintered compact obtained according to the JIS standard. Semi-circular surface cracks of about 100 μm and 200 μm were made on the center of the tension surfaces of three-point bending specimens using a Vickers indenter. After crack-healing processing at 1200 °C and 1300 °C for 1 hr. in air, the cyclic and static fatigue strength behavior of these crack-healed specimens were determined systematically at high temperatures of 800 °C, 1000 °C, 1200 °C, and 1300 °C. The Si<sub>3</sub>N<sub>4</sub>/SiC composite ceramics were shown to possess remarkable crack-healing ability, and the crack-healed specimens showed cyclic and static fatigue strength behavior similar to smooth specimens at high temperatures as well as at room temperature. The crack-healed zones had sufficient fatigue strength even in a high-temperature environment, and most fractures occurred outside the pre-cracked zone in those crack-healed specimens.*

**Keywords:** Si<sub>3</sub>N<sub>4</sub>/SiC ceramics, Crack-healing, Bending strength, Cyclic fatigue strength, Static fatigue strength

## INTRODUCTION

Structural engineering ceramics are widely used in all kinds of engineering fields for their advantages of heatproof property, wear resistance, and corrosion resistance, such as turbo-charger, ceramic gas turbines, auto heat engine, and so on. But it is still a difficulty that ceramics materials were utilized in all kinds of fields more efficiently, because of their machining performance and high cost due to brittleness and low fracture toughness compared with metal materials. However, some engineering ceramics possessing the ability of crack healing were discovered.<sup>1-7</sup> If this ability could be used in engineering ceramics components, their reliability will be increased and

their lifetime will also be prolonged, correspondingly.

We studied the static strength behavior of crack-healed mullite/SiC ceramics,<sup>8,18</sup> Si<sub>3</sub>N<sub>4</sub>/SiC ceramics,<sup>9-12,14,16</sup> and SiC ceramics.<sup>13</sup> We have also verified that the crack-healing ability of Si<sub>3</sub>N<sub>4</sub>/SiC composite ceramics is better than that of monolithic Si<sub>3</sub>N<sub>4</sub> ceramics.<sup>11</sup> Furthermore, we have found that Si<sub>3</sub>N<sub>4</sub>/SiC with Y<sub>2</sub>O<sub>3</sub> as a sintering additive has crack-healing ability under loading.<sup>15,18</sup> We also have reported that the “crack-healing+proof test” method is useful to increase the reliability of ceramic component.<sup>17</sup>

In actual engineering utilization, ceramic components are often operating in a variable load environment, continuously. Consequently, it is very important to make clear the fatigue strength behavior of crack-healed ceramics. This paper focuses on investigating the cyclic fatigue behavior at room and elevated temperature, and the static fatigue behavior at elevated temperature of crack-healed Si<sub>3</sub>N<sub>4</sub>/SiC composite ceramics.

## MATERIAL, SPECIMEN, AND TEST METHOD

In accordance with research findings heretofore, Si<sub>3</sub>N<sub>4</sub>/SiC composite ceramics with Y<sub>2</sub>O<sub>3</sub> powder added as a sintering additive possess the most remarkable crack-healing ability, but it also have a low strength. If Al<sub>2</sub>O<sub>3</sub> powder was also added as a sintering additive at the same time with Y<sub>2</sub>O<sub>3</sub> powder, denser sintering compact could be obtained, and the strength would be improved. However, in the case that Al<sub>2</sub>O<sub>3</sub> powder was added as a sintering additive, the grain boundary phase of the silicon nitride would be non-crystalline, and there is the possibility of a reduction of the high-temperature strength. In this experiment, these two kinds of Si<sub>3</sub>N<sub>4</sub>/SiC composites, which have different sintering additives, were made to investigate their fatigue strength behavior after being crack-healed.

The silicon nitride powder used in this study has the following properties: mean particle size = 0.2  $\mu$  m, the volume ratio of  $\alpha$ -Si<sub>3</sub>N<sub>4</sub> is above 95%, and the rest is  $\beta$ -Si<sub>3</sub>N<sub>4</sub>. The SiC powder used has a 0.27  $\mu$  m mean particle size and the quantity of SiC powder added is 20wt.% in contrast to the Si<sub>3</sub>N<sub>4</sub> powder.

The samples were made with a mixture of silicon nitride, SiC powder, and 8wt% Y<sub>2</sub>O<sub>3</sub> or 5wt.% Y<sub>2</sub>O<sub>3</sub> and 3wt.% Al<sub>2</sub>O<sub>3</sub> as sintering additive powder. To this mixture, alcohol was added and blended completely for 48hr with a nylon ball, after that the mixture was placed in an evaporator to extract the solvent and then in a vacuum desiccator to produce a dry powder mixture. The mixture was subsequently hot-pressed at 1850°C and pressure of 35 MPa for 2h in nitrogen gas, and 5×90×90mm sintered plate was then obtained; SN-SC-Y5A3(SiC: 20wt.%, Y<sub>2</sub>O<sub>3</sub>: 5wt.%, Al<sub>2</sub>O<sub>3</sub>: 3wt.%)

and SN-SC-Y8(A)(B)(C) (SiC: 20wt.%, Y<sub>2</sub>O<sub>3</sub>: 8wt.%). Where the (A), (B), and (C) indicates the specimen that was made from different batches.

The sintered plate was cut into specimens with height, width, and length dimensions of 3 × 4 × 40mm. The surface of the specimen was mirror finished by lapping after surface grinding using by a diamond grindstone of # 600; the surface roughness of the specimen, R<sub>max</sub>, was 0.05 μm.

To elevate the bending strength, a three-point bend test was carried out at a temperatures ranging from room temperature to 1400°C in accordance with JIS 1061. The span length and cross-head-speed were 30 mm and 0.5mm/min, respectively.

A surface crack was made at the center of the tension surface of the specimen with Vickers indenter in order to investigate the strength of a crack-healed zone. Vickers loads was 19.6N and 49N, and the size of surface cracks was about 100 and 200 μm, respectively. The shape of a crack with diameter of about 100 μm is shown in Fig. 1.

The pre-cracked specimens were heated at a rate of 10°C/min, and the time of exposure was 1h for all specimens. Cooling was spontaneous in the furnace. The healing temperature is 1300°C for the SN-SC-Y8 specimen and 1200 °C for the SN-SC-Y5A3 specimen.

Static fatigue tests were performed at 800 and 1000°C in air, and the loading was also three-point bending. The tests were stopped if rupture had not occurred by 10<sup>6</sup> s.

Cyclic fatigue tests were made at temperatures ranging from 800 to 1300°C in air, at a stress ratio R=0.2 and using sine wave with a frequency of 5Hz.

The fracture surfaces were analyzed by optical and scanning electron microscopy (SEM) techniques.

## TEST RESULTS AND DISCUSSION

### *Bending Strength of Crack-Healed Specimen at High Temperatures*

The test temperature dependence of a crack-healed specimen's bending strength is shown in Fig. 2 and three pieces of specimen were used in each

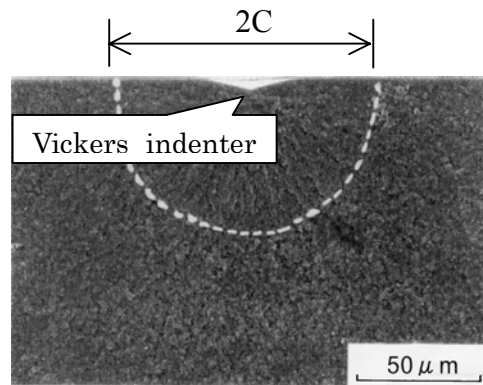


Fig.1 Indented crack shape and fracture surface

condition in the test. In the case of SN-SC-Y8(A), signified by symbol  $\circ$ , the bending strength shows a constant value of 800 MPa up to 1000°C and above 1000°C, about 100MPa lower bending strength showed than that at 1000°C. Moreover, most of the specimens failed outside the crack-healed zone up to 1300°C similar to the crack path shown in Fig. 7(a). In SN-SC-Y8(B) signified by symbol  $\square$ , high bending strength of 850MPa has been shown in 1300°C compared to SN-SC-Y8(A), and all of the specimens ruptured from the outside of the crack-healed zone. However, bending strength was reduced by about 200MPa at 1400°C, and all the specimens ruptured from the pre-crack area. Therefore, the heat resisting limit temperature, in terms of a monotonic load of crack-healed SN-SC-Y8 material is about 1300°C the same as the parent material, and it could be concluded that the healed zone has a enough heat resistance. On the contrary, in the case that the composite SN-SC-Y5A3 containing  $\text{Al}_2\text{O}_3$  signified by symbol  $\blacktriangle$ , the bending strength is almost the same up to 1000°C and the value is about 800MPa. Above 1000 °C , the bending strength decreased dramatically with an increase in the test temperature. Moreover, all specimens ruptured from the crack-healed zone. From these results, it could be concluded that the heat resisting limit temperature in monotonic load is about 1000°C.

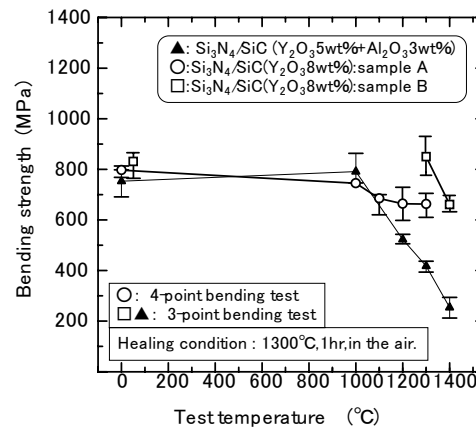


Fig2. Effect of test temperature on strength of crack-healed specimen

### ***Fatigue Strength at High Temperature***

High temperature cyclic fatigue strength of crack-healed specimens was investigated using SN-SC-Y8(C) material, and the test result is shown in Fig. 3. In Fig.3, three-point bending strength at room temperature of the smooth and pre-cracked specimens of SN-SC-Y8(C) was shown on the left side of the dashed line, which signified by symbol  $\circ$  and  $\triangle$ , respectively. The bending strengths of the smooth and pre-cracked specimen is about 600 and 300 MPa, respectively. These values are smaller than that of SN-SC-Y8 (B). Using SEM, the fracture surface of the specimen fractured in bend test was observed, and its photograph is shown in Fig. 4. From this SEM photograph, it can be seen that fracture occurred from a large internal processing flaw in the specimen due to sintering faults. It seems that

abounding existence of these internal flaws is the reason that the three-point bending strength was decreased. By the way, there was no effective difference between SN-SC-Y8 (C) and (B) in the strength on crack-healing behavior. The cycle fatigue tests were stopped at  $N_f=2 \times 10^6$  cycles. The specimens which did not fracture in the test are marked by an arrow symbol( $\rightarrow$ ) in the figure. The  $\sigma_{fc}$  decreased with increasing test temperature to about 600MPa at 1000 °C (●), 550MPa at 1200 °C (▲), and 400MPa at 1300 °C (◆). However, crack-healed SN-SC-Y8 (C) possessed enough cyclic fatigue strength up to 1200°C

in comparison with the smooth specimen's bending strength at RT and not showed any degradation under cyclic fatigue. On the contrary, the  $\sigma_{fc}$  at

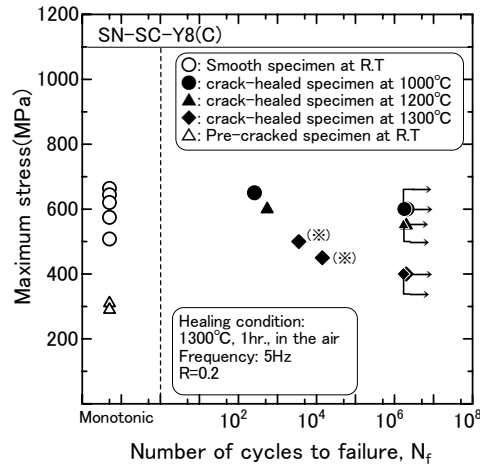


Fig.3 Cyclic fatigue test result of SN-SC-Y8(C) at high temperature

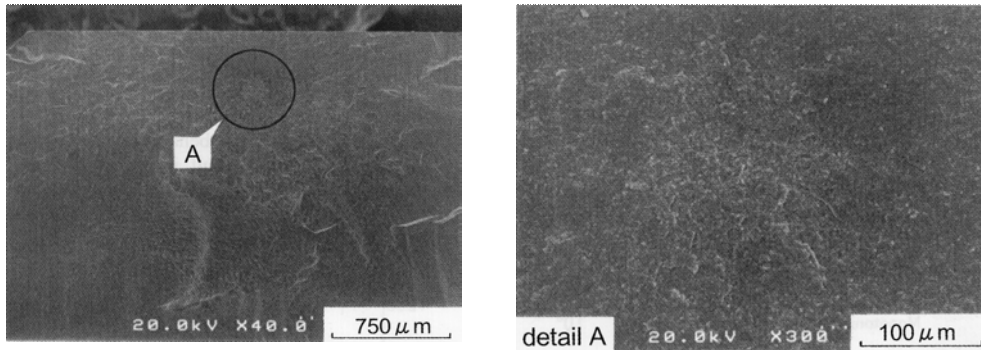


Fig.4 SEM photograph of the fracture surface of the crack-healed SN-SC-Y8 specimen which failed under cyclic load at 1300°C. ( $\sigma_{max}=500$  MPa,  $N_f=3530$  cycles)

1300°C was as low as 400 MPa and, however, all specimens which were failed during the test had been fractured from outside the crack-healed zone. A SEM photograph of the fracture surface is shown in Fig. 4. The fracture initiated from an internal defect in the specimen, not from the crack-healed zone. These results confirm that the heat resisting limit temperature of

crack-healed SN-SC-Y8 material was 1200°C, but the material is no more sensitive to cyclic fatigue up to 1300°C. High-temperature fatigue tests were carried out for the SN-SC-Y5A3 specimen under an ambience of 800°C. The test result is shown in Fig. 5. Figure 5(a) shows the result of the static fatigue test at 800°C, and Fig. 5(b) shows the result of the cyclic fatigue test. The three-point bending strengths at room temperature under static loads for smooth, pre-cracked, and crack-healed specimens are shown on the left side of the dashed line, which signified by symbols ○, △, and ▲, respectively. All of the pre-crack lengths are about 100 μm. The static fatigue tests were stopped at  $t_f=1 \times 10^6$  s. The specimens which did not fracture in the test are marked by an arrow symbol (→) in the figure. The applied stress which a specimen did not fracture up to  $t_f=1 \times 10^6$  s is denoted as  $\sigma_{fs}$ . The  $\sigma_{fs}$  of the SN-SC-Y5A3 specimen at 800°C after crack-healing was about 670MPa. The cyclic fatigue limit ( $\sigma_{fc}$ ) of the SN-SC-Y5A3 specimen at 800°C

after crack-healing is about 600MPa. There were two pieces of specimen, which were marked by an arrow symbol (→), which did not fracture until  $N=2 \times 10^6$  cycles under maximum stress of 600MPa. Using the specimens, a bending test at RT was performed and their bending strength is 1016 and 841 MPa, respectively. SEM photographs of the fracture pattern and the fracture surface are shown in Fig. 6. The fracture occurred from outside of the crack-healed zone, as shown in Fig.6(a). The fracture initiation site is at an internal flaw as shown in Fig. 6(b). From these results, it is concluded that the crack-healed zone had enough strength in both cyclic and static fatigue up to 800°C. The static fatigue strength behavior at 1000°C was investigated, and the test result is shown in Fig. 7. The three-point bending strengths at room temperature of the smooth, as-cracked specimen, and crack-healed specimen, which signified by symbols ○, △, and ▲, are shown on the left side of the dashed line in the figure. From Fig. 6, it can be seen that the

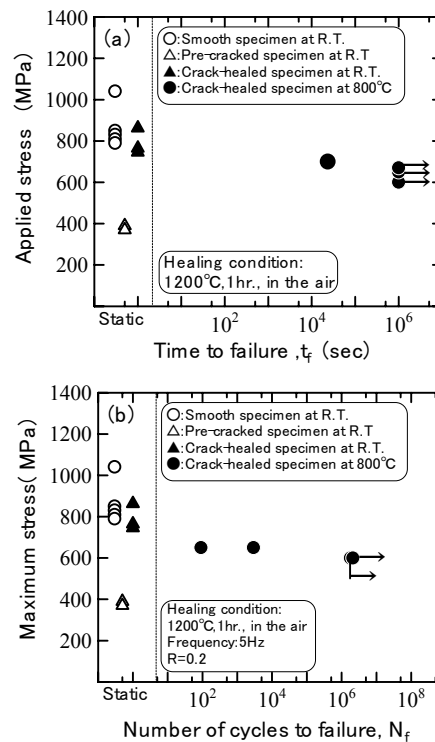


Fig.5 (a)Static fatigue and (b) cyclic fatigue test results of SN-SC-Y5A3 at 800°C

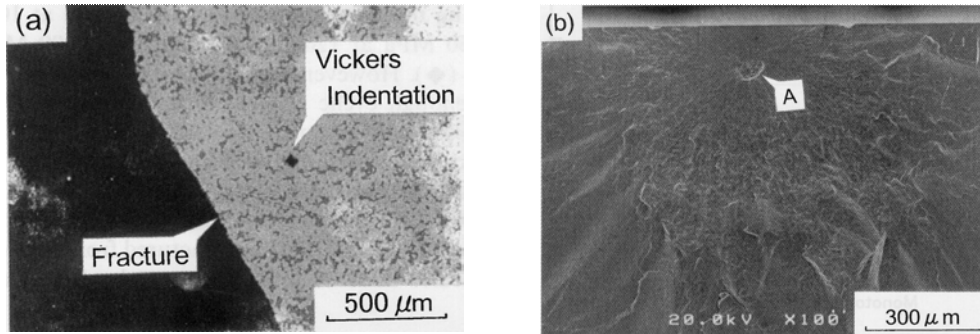


Fig.6 Fracture patterns and (b) fracture initiation site of the crack-healed SN-SC-Y5A3 specimen which survived in the cyclic fatigue test and then was bend-tested at R.T after the cyclic fatigue test of  $N_f=2 \times 10^6$  cycles,  $\sigma_{max}=600$  MPa at  $800^\circ\text{C}$ .

static fatigue limit ( $\sigma_{fs}$ ) of smooth specimens at  $1000^\circ\text{C}$  was about 600MPa, and the  $\sigma_{fs}$  of a crack-healed specimen was about 300MPa, which shows a half value of the smooth specimens. Furthermore, all the specimens that failed during the static fatigue test fractured from the crack-healed zone. Consequently, the crack-healed zone is sensitive to static fatigue at  $1000^\circ\text{C}$ , and the heat-resisting limit temperature on static fatigue of SN-SC-Y5A3 is  $800^\circ\text{C}$ .

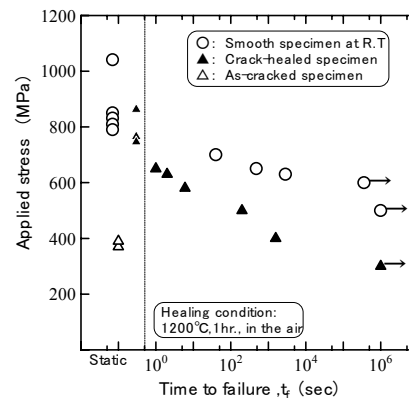


Fig.7 Static fatigue test results of smooth and crack-healed SN-SC-Y5A3 specimen at  $1000^\circ\text{C}$ .

## CONCLUSIONS

The following results were obtained in this study.

1. The heat resisting limit temperature on monotonic load of crack-healed SN-SC-Y8 material is about  $1300^\circ\text{C}$ , as in the parent material.
2. The heat resistance limit temperature of crack-healed SN-SC-Y8 material was  $1200^\circ\text{C}$ , but the material is not sensitive to cyclic fatigue up to  $1300^\circ\text{C}$ .
3. The crack-healed specimen of SN-SC-Y5A3 material is not sensitive to either static or cyclic fatigue up to  $800^\circ\text{C}$ . However, at  $1000^\circ\text{C}$ , the

static fatigue strength decreased dramatically and all that specimens that failed in the test are fractured from the crack-healed zone. Consequently, it could be concluded that the heat resisting limit temperature of SN-SC-Y5A3 on static fatigue is 800°C.

## REFERENCES

1. Petrovic, J.J. and Jacobson, L.A.(1976) *J.Am.Ceram.Soc.* **59**, 34.
2. Gupta, T.K.(1976) *J.Am.Ceram.Soc.* **59**, 259.
3. Choi, S.R. and Tikara, V.(1992) *Scripta Metall Mater.* **26**, 1263.
4. Moffatt, J.E., Plumbridge, W.J. and Hermann, R.(1996) *British Ceramic Trans.* **95**, 23.
5. Chu, M.C., Sato, S., Kobayashi, Y., Ando, K.(1994) *Jpn.Soc.Mech.Engng.* **60-580,A**, 2829.
6. Chu, M.C., Sato, S., Kobayashi, Y., Ando, K.(1995) *Fatigue Fract. Eng. Mater. Struct.* **18-9**, 1019.
7. Sato, S., Chu, M.C., Kobayashi, Y., Ando, K.(1995) *Jpn.Soc.Mech.Engng.* **61-585, A**, 1023.
8. Ando, K., Tsuji, K., Hirasawa, T., Kobayashi, Y., Chu, M.C., Sato, S.(1999) *J.Soc.Mater.Sci., Jpn.* **48-5**, 484.
9. Ando, K., Ikeda, T., Sato, S., Yao, F., Kobayashi, Y.(1998) *Fatigue Fract. Eng. Mater. Struct.*, **21**, 119.
10. Chu, M.C., Ando, K., Sato, S., Hirasawa, T., Kobayashi, Y.(1998) *High Pressure Inst. Jpn.* **36-2**, 82.
11. Ando, K., Chu, M.C., Sato, S., Yao, F., Kobayashi, Y.(1998) *Jpn.Soc.Mech.Engng.* **64-623, A**, 1936.
12. Ando, K., Sato, S., Kobayashi, Y. and Chu, M.C.,(1998), In Fracture from defects, ECF 12, pp.497-502, Brown, M.W., Rios, E.R de los, and Miller, K.J.(Ed.).
13. Koros, Y., Chu, M.C., Nakatani, M and Ando, K.(2000) *J.Am.Ceram.Soc.*, **83-11**, 2788
14. Ando, K., Chu, M.C., Y.Kobayashi, Yao, F., Sato, S.(1999) *Jpn. Soc. Mech. Eng.*, **65-633, A**, 1132.
15. Ando, K., Chu, M.C., Yao, F., Sato, S.(1999) *Fatigue Fract. Eng. Mater. Struct.* **22**, 897.
16. Yao, F., Ando, K., Chu, M.C., Sato, S.(2000) *J.Matls.Sci.(Letts)*. **12(19)**, 1081.
17. Ando, K., Shirai, Y., Nakatani, M., Kobayashi, Y., and Sato, S.(2002) *J. Euro. Ceram. Soc.*, **22-1**, 121
18. Ando, K., Furusawa, K., Chu, M.C., Hanagata, T., Tuji, K., and Sato, S.(2001) *J. Am. Ceram. Soc.*, **84-9**, 2073